Wind and Structures, *Vol. 30, No. 3 (2020) 317-323*
DOI: https://doi.org/10.12989/was.2020.30.3.317

Improvement of dynamic responses of a pedestrian bridge by utilizing decorative wind chimes

Wei-ya Liu[1], Hai-jun Tang[1], Xiaoyue Yang[2a] and Jiming Xie[*2]

[1]OCT Group, Shenzhen 518053, China
[2]Zhejiang University, College of Civil Engineering and Architecture, Hangzhou 310058, China

(Received January 29, 2019, Revised May 7, 2019, Accepted May 9, 2019)

Abstract. A novel approach is presented to improve dynamic responses of a pedestrian bridge by utilizing decorative wind chimes. Through wind tunnel tests, it was verified that wind chimes can provide stabilization effects against flutter instability, especially at positive or negative wind angles of attack. At zero degrees of angle of attack, the wind chimes can change the flutter pattern from rapid divergence to gradual divergence. The decorative wind chimes can also provide damping effects to suppress the lateral sway motion of the bridge caused by pedestrian footfalls and wind forces. For this purpose, the swing frequency of the wind chimes should be about the same as the structural frequency, which can be achieved by adjusting the swing length of the wind chimes. The mass and the swing damping level are other two important and mutually interactive parameters in addition to the swing length. In general, 3% to 5% swing damping is necessary to achieve favorite results. In the study case, the equivalent damping level of the entire system can be increased from originally assumed 1% up to 5% by using optimized wind chimes.

Keywords: wind chimes; pedestrian bridge; aerodynamic stability; flutter; pedestrian-induced motion; wind tunnel tests; control of dynamic response

1. Introduction

Compared to long-span highway bridges, modern pedestrian bridges present different challenges in design. As the aesthetic satisfaction of cultural values is an important factor in pedestrian bridge design, the structures of pedestrian bridges tend to be more slender and sleek to allow them to blend into or enhance the environment (Ingólfsson 2012). However, an unintended consequence is that these slender bridges are often very susceptible to dynamic loads, especially to wind loads and pedestrian-induced loads (Nakamura 2003, Pirner and Fischer 1998, Pirner 1994, Ingólfsson *et al.* 2011, Huang *et al.* 2005, Zall *et al.* 2017).

The newly proposed pedestrian bridge over a valley of Kulen Mountain is a unique structure designed for leisure and recreation walking, using a steel ribbon hanging system. The total 88 m long bridge consists of a 64 m main span and a 24 m side span. Two pre-stressed steel ribbons carry a 2.7 m wide concrete deck over the valley, as shown in Fig. 1.

After a preliminary study, the main design issues were identified, including 1) potential wind-induced aerodynamic instability, and 2) potential lateral motion induced by footfalls, which might cause pedestrian panics.

The bridge is located in a typhoon prone area in South China. Based on statistical analysis on the local wind climate as well as topographic study at the bridge site, the flutter design wind speed was determined to be 50 m/s.

For the intended recreation use of the bridge, although the pedestrian-induced vertical motion is permitted to have a little higher amplitude than common comfort criterion (BS5400 1978, Ma *et al.* 2018), the pedestrian-induced lateral motion, similar to that of the London Millennium Bridge before retrofit (Low *et al.* 2001), has to be controlled. Therefore, a measure needs to be developed to avoid the potential dynamic issues.

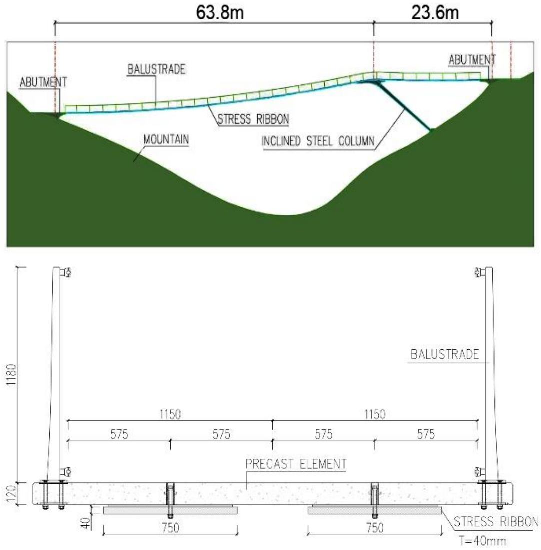

Fig.1 The study bridge

*Corresponding author, Professor
E-mail: jiming_xie@zju.edu.cn
[a] Ph.D. Student
E-mail: xiaoyue_yang@zju.edu.cn

ISSN: 1226-6116 (Print), 1598-6225 (Online)

Fig. 2 Illustration of wind chimes

To improve the aerodynamic stability and suppress the pedestrian-induced bridge motions, conventional approaches are applying shape modifications on the bridge deck and using supplementary damper devices (Ito 1987, Moutinho 2011, Newland 2003, Jiménez-Alonso and Sáez 2018). During the solution development for the excessive lateral motions of the London Millennium Bridge, three kinds of solutions were proposed, stiffening the structure, limiting the number of pedestrians on the bridge, and using supplementary dampers. Although the last one was finally adopted by the bridge designers, these three kinds of solutions represent the available approaches now in dealing with bridge lateral motions. As an alternative approach of limiting the number of pedestrians on the bridge, mitigation through walkway shaping was proposed (Venuti and Bruno 2013). It is also reported that tuned liquid dampers were used to suppress human-induced lateral motions (Yoneda 2014). However, these approaches were not accepted by the design team due to other design constraints.

The decorative wind chimes on both sides of the bridge deck provided a possible solution to solve the problem. The wind chimes were architecturally designed to represent the local cultural heritage, as shown in Fig. 2, and based on the original design, these wind chimes should be removed after receiving windstorm warning.

From structural dynamic point of view, the wind chimes can be considered as sub-structures whose swing may exert counteracting forces to absorb the bridge's lateral motion. From aerodynamic point of view, the wind chimes will affect the flow separation in strong winds and alter the bridge's aerodynamic performance. These potential benefits were investigated in the study.

The results of the study demonstrate a successful example in pedestrian bridge design by using decorative elements for engineering purpose. Details of the study are given below.

2. Effects of wind chimes on aerodynamic stability of the bridge

To validate the effects of wind chimes on bridge's aerodynamic stability, wind tunnel tests were conducted by using 1:10 scale sectional models for two configurations. The first configuration was the basic bridge deck without wind chimes, and the second configuration was the bridge deck with the wind chimes in place, as shown in Fig. 3.

While the conventional similarity principles for sectional models can be applied to the first configuration, an extra similarity requirement, the Froude number similarity, has to be satisfied for the second configuration. This is to correctly simulate the swing of the wind chimes. For simplicity, the scale factors that meet the Froude number similarity (Simiu and Scanlan 1996) were used for both configurations of the sectional models, as given in Table 1.

A structural dynamic analysis was performed to determine the dynamic properties of the bridge, from which the first vertical bending frequency and the first torsional frequency were found to be 0.787 Hz and 0.923 Hz, respectively, and the frequency ratio was 1.17. Based on the scale factors shown in Table 1, the required frequencies of the sectional model were 2.49 Hz and 2.92 Hz for vertical and torsional vibrations, respectively.

(a) Configuration 1 (b) Configuration 2

Fig. 3 Wind tunnel test configurations

Table 1 Scale factors for model design

Quantity	Scale factor (model : full scale)
Length	λ_L= 1:10
Wind velocity	λ_V= 1:$\sqrt{10}$ = 1:3.16
Frequency	λ_ω= 1:$1/\sqrt{10}$ = 1:0.316
Time	λ_t= 1:$\sqrt{10}$ = 1:3.16
Mass/Length	λ_m= 1:10^2 = 1:100
Mass moment/Length	λ_I= 1:10^4 =1:10000
Acceleration	λ_A= 1:1

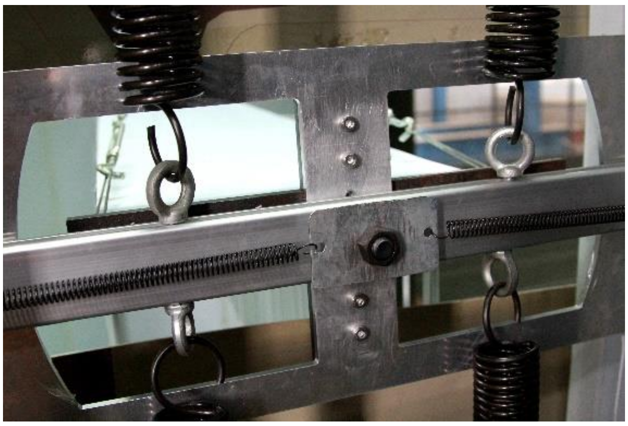

Fig. 4 Spring suspension system of the sectional model

(a) At zero wind speed

(b) At zero wind speed

Fig. 5 Wind tunnel model

Eight custom-built springs, four on each side, were used to provide the required vertical frequency. The torsional frequency was achieved by adjusting the spacing between the springs, as shown in Fig. 4.

The assumed structural damping ratio of 0.5% was obtained by using a damper rod immersed in a viscous liquid cartridge. To ensure the rigidity of the deck, a s tay-cable system was designed and installed on the dec k section that provided sufficient stiffness for bending and twisting but had negligible aerodynamic influences. Fig. 5 shows the study model of Configuration 2.

In general, three types of wind-induced bridge responses need to be considered in bridge design (Xie *et al*. 2006).

• Flutter - a self-excited aerodynamic instability. For the given bridge deck section (Configuration 1 of Fig. 3), if flutter occurs, it will involve coupled torsional and bending motions. Since flutter can grow to very large amplitude of oscillation and cause structural failure, it is important to ensure that the onset wind velocity of flutter instability is sufficiently high. In the study case, the flutter design speed is about 60% higher than the 50-year return period wind speed based on the local design standard.

• Vortex-induced oscillation (VIO) - an oscillation with self-limited amplitude. The vortex-induced oscillation originates from the alternate and regular shedding of vortices from upper and lower edges of the bridge deck. If the frequency of the vortex shedding is close to one of the structural frequencies, resonant motion may occur. The vortex-induced oscillation can be a problem if the amplitude is excessive.

• Buffeting - an unsteady response caused by unsteady wind
loading due to wind turbulence. The buffeting response is often the major contributor to design wind loads for structural system.

It is evident that if only buffeting responses are considered, the structural design loads for Configuration 2 are higher than Configuration 1 due to increased drag force by wind chimes. However, the structural analysis revealed that since the given structural system had sufficient capacity to undertake the increased wind loads, the main challenges in wind-resistant design of the bridge were about the flutter instability and vortex-induced oscillation. The details of buffeting analysis will therefore not be further discussed in this paper.

To examine the aerodynamic stability against flutter and VIO, the wind tunnel tests were first conducted in smooth flow. In smooth flow, the onset wind velocities of flutter and VIO can be clearly identified. The turbulent flow, which can provide more realistic indication of bridge response in natural winds, was tested for further validation of aerodynamic instability. Based on the results of topographic study, the turbulence intensities in strong winds at the bridge deck level were estimated to be 16% in longitudinal direction and 8.5% in vertical direction. The turbulence flow was simulated in wind tunnel by using specially designed upwind spires.

During the tests, the wind speed was gradually increased in small steps and the motions in both vertical and torsional directions were measured by using laser displacement transducers. The wind speed increased until the flutter instability was observed.

Fig. 6 compares the measured motions of the bridge model in two configurations for the wind angles of attack of 0º, +3º and -3º, respectively, where δ_V = standard deviation of vertical motion; δ_T = standard deviation of torsional motion; *D*=deck depth (*D*=160 mm at full scale). A non-dimensional reduced wind velocity *U/fB* was used to present the results, where *U* was the mean wind velocity at the deck level; *f* was the structural bending frequency for reference; and *B* was the deck width (=2700 mm at full scale).

It is evident that the wind chimes did stabilize the bridge against flutter instability, especially in the case of positive or negative wind angles of attack. At the zero angle of attack, although the onset velocities for both configurations were similar, the divergence of flutter became much softened with the wind chimes in place, which was creditable for structural safety. Fig. 6 also indicates that for both configurations, vortex-induced oscillations were not observed during testing. Therefore, vortex-induced oscillations were not considered to be a problem for the bridge.

Fig. 7 illustrates the response of Configuration 2 in turbulent flow. At reduced wind velocity of about 25, the increase of torsional response with increase of wind speed was noticeably accelerated, which is in good agreement with the results from smooth flow tests. Since the

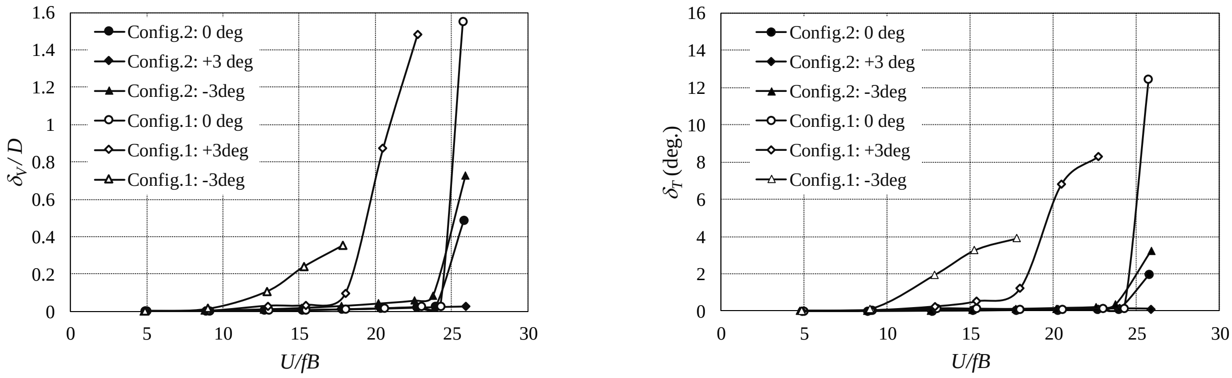

(a) Vertical motion (b) Torsional motion

Fig. 6 Wind-induced bridge motion in smooth flow

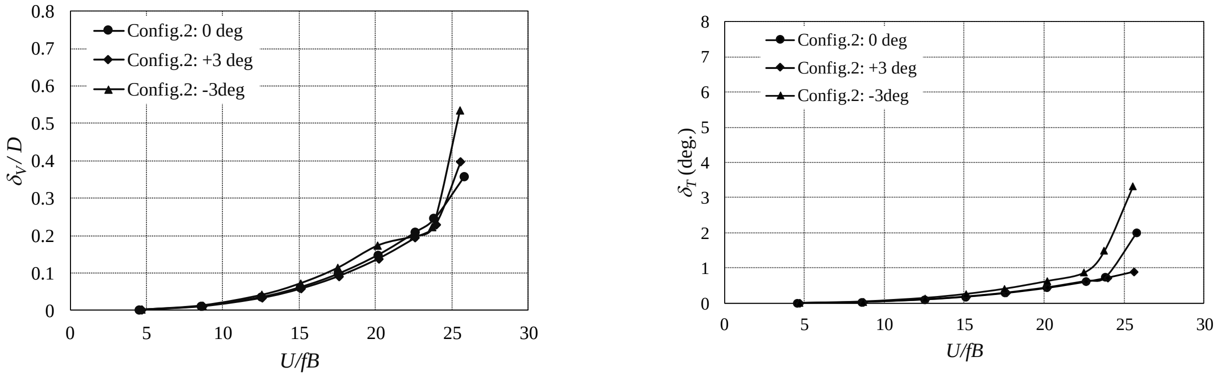

(a) Vertical motion (b) Torsional motion

Fig. 7 Wind-induced bridge motion in turbulent flow

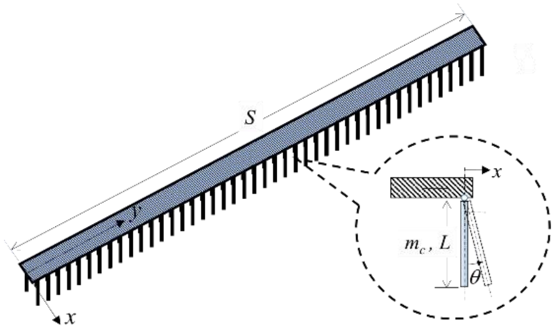

Fig.8 Coordinate system

corresponding onset flutter speed (U=25fB=25×0.787×2.7=53 m/s) exceeded the flutter design speed of 50 m/s in all tested angles of attack, the bridge was considered aerodynamically stable.

For the study bridge, the originally designed wind chimes met the requirements for wind loads and aerodynamic stability. However, in the general application of wind chimes, the wind chimes should be optimized to provide sufficient aerodynamic stabilization while minimizing the increase in drag force. Since the effects of wind chimes are mainly to disrupt flow separations and wake formation, the length of the wind chimes does not need to be very long. The length that satisfies the effective damper requirements, as discussed in the next section would normally be sufficient for aerodynamic improvement.

3. Effects of wind chimes on suppression of lateral motion

To investigate the potential of wind chimes in reducing lateral motions, the coordinate system shown in Fig. 8 was used.

In principle, the wind chimes have potential to suppress bridge deck motion by exerting counteracting forces on bridge deck, similar to tuned mass dampers. However, the parameters of the wind chimes need to be optimized in order to realize this potential benefit. For the study bridge, the objective is to suppress the lateral motion in the fundamental sway mode.

The kinetic and potential energy of the bridge in the fundamental sway mode can be expressed by

$$T_B = \frac{1}{2}\int_0^S m_B(s)\Phi_B^2 \dot{x}^2 ds = \frac{1}{2} M_B \dot{x}^2$$
$$V_B = \frac{1}{2} k x^2 \tag{1}$$

where T_B=kinetic energy; S=bridge span length; m_B=deck mass per length; Φ_B=mode shape of the bridge deck; x=generalized deflection; M_B=generalized mass; V_B=potential energy; k=generalized stiffness given by $k=\omega_B^2 M_B$ where ω_B is the natural frequency of the bridge without wind chimes.

The kinetic and potential energy of each wind chime in swing can be calculated by

$$\tau_C=\int_0^L \frac{1}{2}\left[\left(\Phi_B\dot{x}+\cos(\Phi_C\theta)s\Phi_C\dot{\theta}\right)^2+\left(\sin(\Phi_C\theta)s\Phi_C\dot{\theta}\right)^2\right]\frac{m_c}{L}ds$$
$$\approx\frac{1}{2}m_c\Phi_B^2\dot{x}^2+\frac{1}{6}m_c\left(L\Phi_C(y)\dot{\theta}\right)^2+\frac{1}{2}m_c\Phi_B\Phi_C\dot{x}\left(L\dot{\theta}_y\right) \qquad (2)$$
$$v_C=\int_0^L\left(1-\cos(\Phi_C\theta)\right)\frac{m_c}{L}gsds\approx\frac{1}{4}\Phi_C^2 m_c gL\theta^2$$

where Φ_C= mode shape of the wind chimes; m_c= mass of each chime; L= length of each chime, shown in Fig. 8.

The summation of Eq. (2) for all wind chimes gives the total energy of the wind chimes.

Based on the principle of Lagrange equation, the equations of motion of the bridge-chimes system can be written as

$$\left.\begin{aligned}&M_B\ddot{x}+M_C\gamma_1\ddot{x}+\frac{1}{2}M_C\gamma_2 L\ddot{\theta}+M_B\omega_B^2 x=F\\&\frac{1}{3}M_C L^2\ddot{\theta}+\frac{1}{2}M_C\gamma_2 L\ddot{x}+\frac{1}{2}M_C gL\theta=0\end{aligned}\right\} \qquad (3)$$

where $M_C=m_c\sum\Phi_C^2$ =generalized mass of total wind chimes; $\gamma_1=\sum\Phi_B^2/\Phi_C^2$; $\gamma_2=\sum\Phi_B\Phi_C/\Phi_C^2$; and F=the generalized force on the bridge. For the fundamental sway mode, we can assume $\gamma_1\approx\gamma_2\approx 1$. By normalizing Eq. (3) by the generalized mass and introducing damping terms in the equations, the equations of motion can be rewritten by

$$\left.\begin{aligned}&(1+\mu)\ddot{x}+2\zeta_B\omega_B\dot{x}+\omega_B^2 x+\frac{1}{2}\mu L\ddot{\theta}=f_B\\&\ddot{\theta}+2\zeta_C\omega_C\dot{\theta}+\omega_C^2\theta+\frac{3}{2L}\ddot{x}=0\end{aligned}\right\} \qquad (4)$$

where $\mu=M_C/M_B$=mass ratio between the wind chimes and the bridge; $\omega_C=\sqrt{3g/2L}$=natural frequency of the wind chimes; and $f_B=F/M_B$.

The transfer functions for bridge motion and for chime's swing can thus be determined by

$$\begin{aligned}&\left|H_x(i\omega)\right|^2=\frac{1}{E}\left[\left(1-\left(\frac{\omega}{\omega_C}\right)^2\right)^2+4\zeta_C^2\left(\frac{\omega}{\omega_C}\right)^2\right]\\&\left|H_\theta(i\omega)\right|^2=\frac{1}{E}\left[\frac{1}{4}\mu^2L^2\left(\frac{\omega}{\omega_C}\right)^4\right]\end{aligned} \qquad (5)$$

where

$$E=\omega_B^4\left\{\begin{aligned}&\left[\left[\left(1-(1+\mu)\left(\frac{\omega}{\omega_B}\right)^2\right)\left(1-\lambda^2\left(\frac{\omega}{\omega_B}\right)^2\right)-\frac{3}{4}\mu\lambda^2\left(\frac{\omega}{\omega_B}\right)^4-4\zeta_B\zeta_C\lambda\left(\frac{\omega}{\omega_B}\right)^2\right]^2\right.\\&\left.+4\left(\frac{\omega}{\omega_B}\right)^2\left[\zeta_C\lambda\left(1-(1+\mu)\left(\frac{\omega}{\omega_B}\right)^2\right)+\zeta_B\left(1-\lambda^2\left(\frac{\omega}{\omega_B}\right)^2\right)\right]^2\right]\end{aligned}\right.$$

$\lambda=\omega_B/\omega_C$=frequency ratio.

In comparison, the transfer function of the bridge without wind chimes is given by

$$\left|H_x^0(i\omega)\right|^2=\frac{1}{\omega_B^4\left[\left(1-\left(\frac{\omega}{\omega_B}\right)^2\right)^2+4\zeta_B^2\left(\frac{\omega}{\omega_B}\right)^2\right]} \qquad (6)$$

For performance evaluation, the acceleration is normally taken as the indicator which is dominated by its resonance component in case of severe bridge motions. Therefore, the acceleration can be estimated by the following expression.

$$\sigma_{\ddot{x}}^2=\int_0^\infty\omega^4\left|H_x^0(i\omega)\right|^2 S_{f_B}(\omega)d\omega\approx\frac{\omega_B}{8\zeta_B}S_{f_B}(\omega_B) \qquad (7)$$

The relationship between the acceleration and the structural damping shown in Eq. (7) can be used to estimate the effects of the wind chimes in suppression of motions, where S_{f_B} is the pedestrian load spectrum. We define the equivalent damping ratio of the bridge-chime system as follows

$$\zeta_E=\left(\frac{\int\omega^4\left|H_x^0(i\omega)\right|^2 S_{f_B}(\omega)d\omega}{\int\omega^4\left|H_x(i\omega)\right|^2 S_{f_B}(\omega)d\omega}\right)\cdot\zeta_B \qquad (8)$$

The numerator of the right side of Eq. 8 represents the acceleration variance of the bridge with no wind chimes and the denominator gives the acceleration variance of the bridge with wind chimes.

It is apparent that the objective is to maximize the equivalent damping by optimizing the wind chime designs.

In use of pedestrian load spectrum (Bassoli *et al.* 2018) for the integration of Eq. (8), it can be assumed that the frequency of lateral excitations is half of the vertical one.

It should be noted that Eq. (8) can also be used to assess the equivalent damping for lateral wind excitations. Since the lateral wind load spectrum has a much wide band compared to the transfer functions (Simiu and Scanlan 1996), the wind load spectrum $S_{f_B}(\omega)$ in the integration of Eq. 8 can be replaced by $S_{f_B}(\omega_B)$. As such, the integration of Eq. (8) is simplified to involve the integration of transfer functions only.

The mechanic properties of the wind chimes can be described by three parameters: length of each chime L, the mass of each chime m_c, and the swing damping of the chime ζ_C. To perform parameter analysis to optimize the wind chimes for bridge motion reductions, the frequency ratio λ was used to present the parameter L since the nature frequency of the swing is solely determined by the length. The mass of the chime is presented by mass ratio μ.

Fig. 9 shows the equivalent damping ratio of the entire system (bridge structure plus chimes) as a function of frequency ratio. It shows that to use the wind chimes for bridge motion reductions, the swing frequency of the chime should be about the same as the bridge frequency, so that the optimal length of the chime is given by

$$L = \frac{3g}{2\omega_B^2} \tag{9}$$

Fig. 10 shows the equivalent damping ratio as a function of mass ratio. It indicates that although the equivalent damping increases with the increase of the mass ratio, the efficiency largely depends on the swing damping. For example, if the swing damping is very small, say only 0.5%, increase of mass ratio from 1% to 6% only results in an increase of the equivalent damping ratio from 1.4% to 1.5%. However, if the swing damping is 5%, the increase of mass ratio from 1% to 6% will result in an increase of the equivalent damping ratio from 2.7% to 4.4%.

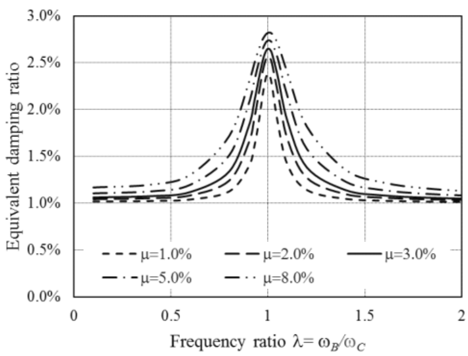

Fig. 9 Equivalent damping ratio as a function of frequency ratio (ζ_B =1%, ζ_C =2%)

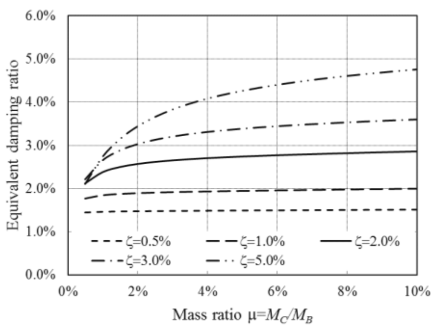

Fig. 10 Equivalent damping ratio as a function of mass ratio (ζ_B =1%, ζ_C =ζ, λ =1.0)

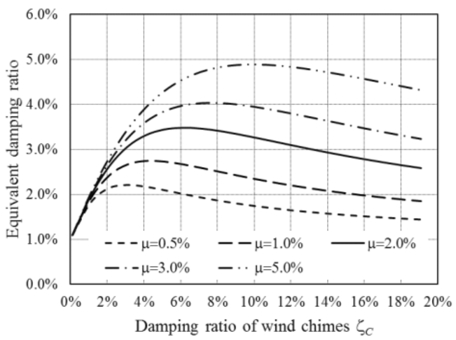

Fig. 11 Equivalent damping ratio as a function of swing damping (ζ_B =1%, λ =1.0)

Fig. 11 further indicates the importance of swing damping in the design of wind chimes. The optimal value of the swing damping depends on the mass ratio. For small mass ratio of 0.5%, the optimal swing damping is about 3% and the maximum equivalent damping can reach to 2.2%. If the mass ratio is 5%, the maximum reachable equivalent damping can be 4.9% at the swing damping ratio of 10%.

Based the above analysis, the optimization procedure of wind chimes for bridge motion reduction can be summarized as follows:

• Step 1: Select the length of the wind chimes by using Eq. (9);

• Step 2: Choose slightly heavier wind chimes if other design requirements permit; and

• Step 3: Add damping to the wind chime swing, such as by increasing the stickiness at the hanging point.

Step 2 and Step 3 require several iterations to reach the optimal values.

In practical applications, the effectiveness of wind chimes as supplementary damping devices is mainly limited by the achievable level of swing damping, while the mass ratio can be readily adjusted. For conventional suspension system, the swing damping ratio is about 2% to 3%, so the achievable equivalent damping ratio is up to 3.5%, shown in Fig. 11. For higher damping ratios, a more sophisticated suspension system is required, which can result in a cost increase.

To improve the dynamic responses of the pedestrian bridge, little conflicts were found in the optimization of wind chimes between the objective of aerodynamic stability and the objective of equivalent damping. For aerodynamic stability, one of the key parameters of the wind chimes is the spacing between the wind chimes because it affects the fluid separation and the wake formation. For equivalent damping effect, one of the key parameters of the wind chimes is the length to achieve a required frequency. The weights of wind chimes are beneficial for both aerodynamic stability and equivalent damping effects.

The wind chimes were made of stainless steel pipes with a diameter of 60 mm for each. In original design, the length of chimes was up to 5m and the mass ratio up to 7%. After optimization with project costs in mind, the length of the chimes was adjusted to 0.6 m with 0.3 m spacing between the chimes and the mass ratio was set at 2%, resulting in an equivalent damping ratio of 3%. Although the equivalent damping ratio can reach 5%, it is found that 3% is sufficient to meet the design objectives with a benefit of low cost.

4. Conclusions

• It is feasible to improve the dynamic responses by utilizing decorative wind chimes on the pedestrian bridge.

• Based on wind tunnel studies, the wind chimes can provide stabilization effects against flutter instability. This is particularly evident for the cases with positive or negative angles of attack. At zero angle of attack, the wind chimes change the flutter pattern from rapid divergence to gradual divergence.

• The drawback of using wind chimes is the increase of drag forces. It is therefore necessary to conduct a case-by-case study in practical applications to determine the optimal size of the wind chimes that can provide sufficient effects on aerodynamic stabilization while maintaining the drag force within an acceptable range.
• Wind chimes can also be optimized to suppress lateral motion induced by pedestrian footfalls or lateral wind forces.
• To use the wind chimes for motion reductions, the swing frequency of the wind chimes should be about the same as the structural frequency, which can be achieved by adjusting the swing length of the wind chimes.
• The chime mass and the swing damping level are two mutually interactive parameters in optimization. In general, 3% to 5% swing damping is necessary to achieve favorite results.
• For the study case, the equivalent damping level of the entire system (bridge and chimes) can be increased from originally assumed 1% up to 5% by using optimized wind chimes.
• Although the study shown in the paper is case-specific, the novel idea of using decorative elements to improve dynamic responses can be a useful reference for pedestrian bridge designs.

References

Bassoli, E., Van Nimmen, K., Vincenzi, L. and Van den Broeck, P. (2018), "A spectral load model for pedestrian excitation including vertical human-structure interaction", *Eng. Struct.*, **156**, 537-547. https://doi.org/10.1016/j.engstruct.2017.11.050.

BS5400 (1978), "Vibration serviceability requirements for foot and cycle track bridges", Part 2, Appendix C, British Standards Institution.

Huang M.H., Thambiratnam D.P. and Perera N.J. (2005) "Vibration characteristics of shallow suspension bridge with pre-tensioned cables", *Eng. Struct.*, **27**(8), 1220-1233. https://doi.org/10.1016/j.engstruct.2005.03.005.

Ingólfsson, E.T., Georgakis, C.T., Ricciardell, F. and Jonsson, J. (2011), "Experimental identification of pedestrian-induced lateral forces on footbridges", *J. Sound Vib.*, **330**(6) 1265-1284. https://doi.org/10.1016/j.jsv.2010.09.034.

Ingólfsson, E.T., Georgakis, C.T. and Jonsson, J. (2012), "Pedestrian-induced lateral vibrations of footbridges: a literature review", *Eng. Struct.*, **45**, 21-52. https://doi.org/10.1016/j.engstruct.2012.05.038.

Ito, M. (1987), "Measures against wind-induced vibrations of bridges", *Bridges and Transmission Line Structures. ASCE*.

Jiménez-Alonso, J.F. and Sáez, A. (2018), "Motion-based design of TMD for vibrating footbridges under uncertainty conditions", *Smart Struct. Syst.*, **21**(6), 727-740. https://doi.org/10.12989/sss.2018.21.6.727

Low, A., Ridsdill Smith, R.M., Willford, M., Dallard, P., Fitzpatrick, A.J., Flint, A., *et al.* (2001), "The London Millennium footbridge", *Structural Engineer*, **79**(171), 17-33.

Ma, R., Ke, L., Wang D., Chen, A. and Pan, Z. (2018). "Experimental study on pedestrians' perception of human-induced vibrations of footbridges", *Int. J. Struct. Stab. Dynamics*, **18**(10), 1-10. https://doi.org/10.1142/S021945541850116X.

Moutinho, C., Cunha, A. and Caetano, E. (2011), "Analysis and control of vibrations in a stress-ribbon footbridge", *Struct. Control Health Monit.*, **18**, 619-634.

Nakamura, S.I. (2003), "Field measurements of lateral vibration on a pedestrian suspension bridge". *Structural Engineer*, **81**(22), 22-26.

Newland D.E. (2003). "Vibration of London Millennium Bridge: cause and cure", *Int. J. Acoust. Vib*., **8**(1), 9-14.

Pirner, M. and Fischer, O. (1998), "Wind-induced vibrations of concrete stress-ribbon footbridges", *J. Wind Eng. Ind. Aerod.*, **74-76**, 871-881. https://doi.org/10.1016/S0167-6105(98)00079-8.

Pirner, M. (1994), "Aeroelastic characteristics of a stressed ribbon pedestrian bridge spanning 252 m", *J. Wind Eng. Ind. Aerod.*, **53**(3), 301-314. https://doi.org/10.1016/0167-6105(94)90088-4.

Simiu, E. and Scanlan, R.H. (1996), *Wind Effects on Structures, 3rd ed.*, John Wiley & Sons, New York, NY, USA.

Venuti, F. and Bruno, L. (2013), "Mitigation of human-induced lateral vibrations on footbridges through walkway shaping", *Eng. Struct.*, **56**, 95-104. https://doi.org/10.1016/j.engstruct.2013.04.019.

Xie, J., Hunter, M. and Irwin, P. (2006), "Experimental and analytical approaches in wind engineering studies for bridges", *Proceedings of the IABSE Symposium on "Responding to Tomorrow's Challenges in Structural Engineering*", Budapest, Hungary, September.

Yoneda, M. (2014), "Human-induced lateral vibration on existing pedestrian suspension bridge and suppression with tuned liquid dampers", *J. Japan Society of Civil Engineers, Ser. A1 (Structural Engineering & Earthquake Engineering (SE/EE))*, **70**, 221-226.

Zall, E. Andersson, A., Ulker-Kaustella, M. and Karoumi, R. (2017), "An efficient approach for considering the effect of human-structure interaction on footbridges", *Procedia Eng.*, **199**, 2913–2918. https://doi.org/10.1016/j.proeng.2017.09.337.

CC